JOURNAL OF Applied Polymer SCIENCE

New Amphiphilic Sulfonic Acid Dopant-Cum-Templates for Diverse Conducting Polyaniline Nanomaterials

Shekhar D. Shinde, M. Jayakannan

Department of Chemistry, Indian Institute of Science Education and Research (IISER), 900, NCL Innovation Park, Dr. Homi Bhabha Road, Pune 411 008, Maharashtra, India

Correspondence to: M. Jayakannan (E-mail: jayakannan@iiserpune.ac.in)

ABSTRACT: We report new structurally identical polar head amphiphilic sulfonic acids as molecular templates to study the role of the polymerization routes on the solid state properties of polyaniline nanomaterials. Three long chain substituted phenols such as 3-pentadecylphenol, renewable resource-cardanol, and nonyl phenol are reacted with sultones to make new long tail amphiphiles. The amphiphilic molecules self-organized as 4–6 nm tiny micelles in water which were employed as templates for polymerization. Emulsion, dispersion, and interfacial polymerization of aniline along with these new amphiphiles produced well-defined polyaniline nanofibers, nanotapes, and nanospheres. Electron microscopic analysis revealed that the dopant structure and polymerization routes determine the morphology of the polyaniline nanomaterials. Absorbance studies revealed that the samples produced via interfacial route showed expanded polymer chain conformation as a result of unidirectional growth of the chains in the aqueous-organic interface. Emulsion and dispersion route samples were produced in coil-like chain conformation. Powder X-ray analysis confirmed that the expanded conformation in the polyaniline backbone enhances the high solid state ordering, high percent crystallinity, and larger crystallite size compared to that of the samples with coil-like conformation. Highly ordered interfacial route samples showed conductivity three orders of magnitude higher than that of the weakly packed polyaniline nanomaterials. © 2012 Wiley Periodicals, Inc. J. Appl. Polym. Sci. 000: 000–000, 2012

KEYWORDS: conducting polymers; self-organization; solid state properties; structure-property correlation; polyaniline; nanomaterials

Received 17 August 2011; accepted 13 April 2012; published online
DOI: 10.1002/app.37880

INTRODUCTION

One- and three-dimensional conducting polymer nanomaterials have been widely attracted for applications in solid-state electrolytes, chemical and biosensors, optoelectronic devices, hydrogen storage, and so on.[1–4] Control of size and shape of these nanomaterials have gained wide attention due to their superior surface and electron transport properties.[5] Among the various conducting polymers, polyaniline and polypyrrole nanomaterials possessed excellent thermal and environmental stability.[6] Synthesis of the conducting polyaniline nanomaterials were reported using hard template approaches like anodic alumina, porous silica, electro spinning methods, and also using soft template approaches like surfactants, gels, lipids, liquid crystals, etc.[7–18] In the soft template approach, micellar mediated polymerization process attained high importance due to the formation of predictable size, shape, and properties of the nanomaterial. Among the surfactants templates, anionic surfactants are very unique in the sense that they act as both template and dopant for polymer nanomaterials.[6] The permanent electrostatic binding of the long-chain anionic surfactants improves the solubility, colloidal stability, conductivity, and solid state packing of the polyaniline nanomaterials.[6] Anionic sulfonic acid consisting of aromatic units and alkyl chains were reported as dopants for conducting polyaniline nanomaterials.[19–22] Recently, we have reported renewable resource based amphiphilic azobenzene sulfonic acid for polyaniline,[23] polypyrrole,[24] and poly (aniline-co-pyrrole) nanomaterials.[25] Though, individual polymerization methodologies such as emulsion,[26,23g] interfacial[1a,27–31] and dispersion routes[32,33] were reported for polyaniline nanostructures, only very few efforts have been taken to understand the role of the particular type of anionic surfactant(s) on the different polymerization routes in water.[34,23d] This partially associated with the nonavailability of the single amphiphilic dopant which could template for more than one polymerization routes under identical conditions. For example, an emulsion friendly dopant like dodecyl benzene sulfonic acid is found not suitable

candidate for interfacial route and vice-versa. This hampered the deep understanding of the role of the structural design of dopant molecules on the polymerization routes. Therefore, it is very important to design new amphiphilic dopants with rational structural design and use them as templates for various types of polymerization routes. This is particularly important because different shape and size of the nanostructures could be obtained without changing the chemical composition of the starting materials. Further, this may facilitate the fundamental understanding of the role of the dopant templates on the different polymerization routes and also provide opportunity for developing new conducting polymer nanomaterial for applications in electrical and optoelectronics.

The present investigation emphasized to address the above issue by designing structurally different six new amphiphilic sulfonic acids and subjects them as templates for various polymerizations routes such as emulsion, interfacial, and dispersion in water. All the dopants were synthesized by adopting common synthetic strategy that ring opening of cyclic sultones by long chain substituted phenols. The structure of the dopant molecules vary in three different ways: (i) number of carbon atoms in the hydrophobic alkyl chains, (ii) unsaturation in the hydrophobic alkyl chains, and (iii) position of alkyl chain attachment in the aromatic ring. For this purpose, three different phenols with long alkyl chain substitution are chosen based on pentadecylphenol, cardanol, and nonylphenol. Butyl and propyl sultones are used as sulfonic acid sources which provide variation in the dopant structures by number of carbon atoms between the aryl-ring to sulfonic acid polar heads. All six new dopants were found soluble in water and their self-organized structures were exploited as molecular templates for polyaniline nanomaterial synthesis. The molecular self-organization of the dopant molecules were analyzed by dynamic light scattering (DLS), zeta potential, and surface tension techniques. DLS and electron microscopes [scanning electron microscope (SEM) and transmission electron microscope (TEM)] analysis were used to study the morphology and also to study their polymerization mechanism. It was found that the structure of the dopant and polymerization routes played major roles in determining the morphology, solid state ordering, and bulk conductivity of the polymer samples. The polymerization methodologies played a major role on the formation of expanded or coil-like chain conformation, which is the main driving force for enhanced solid state ordering and associated conductivity behaviors. In short, by carefully designing the structure of the dopants and polymerization route, we could establish the role on the dopant structures and polymerization routes on the characteristics of conducting polymer nanomaterials, more specifically polyanilines.

EXPERIMENTAL SECTION

Materials

3-Pentadecylphenol, nonyl phenol, 1,4-butanesultone, 1,3-propanesultone, potassium tertiary butoxide, aniline, and ammonium persulfate (APS) were purchased from Sigma Aldrich chemicals. Cardanol was purified by double distillation under vacuum and further passed through silica gel column.

Measurements

Nuclear magnetic resonance (NMR) spectra of the compounds were recorded using 400-MHz Brucker NMR spectrophotometer in d_6-DMSO containing small amount of trimethylsilane (TMS) as internal standard. Infrared spectra of the polymers were recorded using Thermo-Scientific Nicolet 6700 Fourier transform infrared (FT-IR) spectrophotometer in the range of 4000–400 cm^{-1}. Size and zeta potential was recorded using Malvern zetasizer ZS90 instrument. For SEM measurements, polymer samples were subjected for thin gold coating using JEOL JFC-1200 fine coater. The probing side was inserted into JEOL JSM-6360A scanning electron microscope for taking photographs. TEM images were recorded using a Technai-300 instrument. For TEM measurements, the water suspension was prepared under ultrasonic and deposited on Formvar coated copper grid. Wide angle X-ray diffractions (WXRDs) of the finely powdered polymer samples were recorded by Bruker using CuK-alpha emission. The spectra were recorded in the range of $2\theta = 3$–50 and analyzed using TOPAS software. For conductivity measurements, the polymer samples were pressed into a 10-mm diameter disc and analyzed using a Keithley four probe conductivity instrument by applying a constant current. Absorption spectra of the polyaniline (PANI) in distilled water were recorded using Perkin Elmer Lambda-45 UV-VIS Spectrophotometer. Surface tension measurements were performed for all six amphiphilic dopants by using Nima Langmuir-Blodgett isotherm.

Synthesis of 4-(3-Pentadecylphenoxy)butane-1-sulfonic acid (PDP-C4)

3-Pentadecylphenol (5.0 g, 16.5 mmol) was added into a flask containing potassium tertiarybuoxide (3.7 g, 33.0 mmol) in dry ethanol (50 mL). This solution was heated at 60°C for 30 min under nitrogen atmosphere. The contents were cooled and 1,4-butanesultone (4.5 g, 33.0 mmol) was added dropwise. The reaction was continued by refluxing for 40 h under nitrogen atmosphere. It was cooled and white solid mass was isolated by suction filtration. The white potassium salt of the product was suspended in water (20 mL) and acidified by 5 M HCl to get sulfonic acid as white precipitate. The solid was further purified by passing through silica gel column using 15/85 methanol/dichloromethane (DCM) (v/v) as eluent. Yield = 6.9 g (96%). Melting point: 79–83°C. ^{1}H NMR (d_6-DMSO) δ: 7.14 ppm (t, 1H, Ar—H), 6.70 ppm (m, 3H, Ar—H), 3.90 ppm (t, 2H, Ar—O—CH_2), 2.50 ppm (t, 2H, HO_3S—CH_2), 1.72 ppm (m, 4H, —CH_2— CH_2—CH_2—SO_3H), 2.49 ppm (m, 2H, Ar—CH_2—$C_{14}H_{29}$), 1.25 ppm (m, 24H, aliphatic side chain), and 0.84 ppm (t, 3H, —CH_3). ^{13}C NMR (d_6-DMSO) δ: 158.7, 143.9, 129.2, 120.4, 114.4, 111.5, 67.1, 51.1, 35.2, 31.35, 29.1, 28.7, 22.1, 21.9, and 14.0. FT-IR (KBr): 3490, 2916, 2849, 1612, 1581, 1471, 1450, 1296, 1245, 1158, 1058, 969, 864, 778, 752, 718,688, 621, 595, and 529. MALDI-TOF-TOF (MW: 440.0): m/z = 479.1 (as MK^+ ion).

Synthesis of 3-(3-Pentadecylphenoxy)propane-1-sulfonic acid (PDP-C3)

1,3-propanesultone (4.0 g, 33.0 mmol) was ring opened by 3-pentadecylphenol (5.0 g, 16.5 mmol) in presence of base potassium tertiarybuoxide (3.7 g, 33.0 mmol) in dry ethanol (50 mL) following the reaction procedure described for

PDP-C4. The crude solid was purified by passing through a silica gel column using 15/85 methanol/DCM as eluent. Yield = 6.6 g (94%). Melting point: 77–80°C. ^{1}H NMR (d_6-DMSO) δ: 7.14 ppm (t, 1H, Ar—H), 6.71 ppm (m, 3H, Ar—H), 4.00 ppm (t, 2H, Ar—O—CH_2), 2.50 ppm (t, 2H, HO_3S—CH_2), 1.96 ppm(q, 2H, —CH_2—CH_2—CH_2—SO_3H), 2.49 ppm (m, 2H, Ar—CH_2—$C_{14}H_{29}$), 1.25 ppm (m, 24H, aliphatic side chain), and 0.84 ppm (t, 3H, —CH_3). ^{13}C NMR (d_6-DMSO) δ: 158.7, 143.9, 129.1, 120.4, 114.4, 111.5, 66.1, 48.1, 35.3, 31.3, 31.0, 29.1, 28.9, 28.1, 25.1, 22.1, and 14.0. FT-IR (KBr): 3544, 3479, 2916, 2853, 1618, 1579, 1471, 1471, 1445, 1298, 1246, 1183, 1061, 970, 869, 774, 749, 723, 690, 684, 621, 588, and 524. MALDI-TOF-TOF (MW: 426.65): m/z = 465.1 (as MK^+ ion).

Synthesis of (Z)-4-(3-Pentadec-8-enyl)phenoxy) butane-1-sulfonic acid (CAR-C4)

1,4-butanesultone (4.5 g, 33.0 mmol) was ring opened by Cardanol (5.0 g, 16.5 mmol) in presence of base potassium tertiarybuoxide (3.7 g, 33.0 mmol) in dry ethanol (50 mL) following the reaction procedure described for PDP-C4. The crude solid was purified by passing through a silica gel column using 15/85 methanol/DCM as eluent. Yield = 3.0 g (41%). Melting point: 56–62°C. ^{1}H NMR (d_6-DMSO) δ: 7.14 ppm (t, 1H, Ar—H), 6.71 ppm (m, 3H, Ar—H), 5.35 ppm (b, 2H, —CH=HC—), 4.00 ppm (t, 2H, Ar—O—CH_2), 2.50 ppm (t, 2H, HO_3S—CH_2), 1.96 ppm(q, 2H, —CH_2—CH_2—CH_2—SO_3H), 2.49 ppm (m, 2H, Ar—CH_2—$C_{14}H_{29}$), 1.25 ppm (m, 16H, aliphatic side chain), and 0.84 ppm (t, 3H, —CH_3). ^{13}C NMR (d_6-DMSO) δ: 158.7, 143.9, 129.1, 120.4, 114.4, 111.5, 66.1, 48.1, 35.3, 31.3, 31.0, 29.1, 28.9, 28.1, 25.1, 22.1, and 14.0. FT-IR (KBr): 3492, 2916, 2849, 1649, 1581, 1450, 1353, 1284, 1177, 1057, 967, 873, 796, 753, 688, 621, and 525. MALDI-TOF-TOF (MW: 438.66): m/z = 477.0 (as MK^+ ion).

Synthesis of (Z)-3-(3-Pentadec-8-enyl)phenoxy) propane-1-sulfonic acid (CAR-C3)

1,3-propanesultone (4.0 g, 33.0 mmol) was ring opened by Cardanol (5.0 g, 16.5 mmol) in presence of base potassium tertiarybuoxide (3.7 g, 33.0 mmol) in dry ethanol (50 mL) following the reaction procedure described for PDP-C4. The crude solid was purified by passing through a silica gel column using 15/85 methanol/DCM as eluent. Yield = 3.2 g (46%), Melting point: 54–60°C. ^{1}H NMR (d_6-DMSO) δ: 7.14 ppm (t, 1H, Ar—H), 6.71 ppm (m, 3H, Ar—H), 5.31 ppm (b, 2H, —CH=HC—), 4.00 ppm (t, 2H, Ar—O—CH_2), 2.50 ppm (t, 2H, HO_3S—CH_2), 1.96 ppm(b, 2H, —CH_2—CH_2—CH_2—SO_3H), 1.95 (b, 4H, —CH_2—CH=CH—CH_2—), 2.49 ppm (m, 2H, Ar—CH_2—$C_{14}H_{29}$), 1.25 ppm (m, 16H, aliphatic side chain), and 0.84 ppm (t, 3H, —CH_3). ^{13}C NMR (d_6-DMSO) δ: 158.7, 143.9, 130.1, 129.5, 120.3, 114.4, 111.5, 66.1, 47.9, 35.3, 29.1, 28.7, 25.3, 22.1, and 13.9. FT-IR (KBr): 3544, 3479, 2916, 2853, 1618, 1579, 1471, 1471, 1445, 1298, 1246, 1183, 1061, 970, 869, 774, 749, 723, 690, 684, 621, 588, and 524. MALDI-TOF-TOF (MW: 424.64): m/z = 447.1 (as MNa^+ ion).

Synthesis of 4-(2-nonylphenoxy)butane-1-sulfonic acid (NON-C4)

1,4-butanesultone (6.2 g, 45.4 mmol) was ring opened by Nonyl phenol (5.0 g, 22.7 mmol) in presence of base potassium tertiarybuoxide (5.1 g, 45.4 mmol) in dry ethanol (50 mL) following the reaction procedure described for PDP-C4. The crude solid was purified by passing through a silica gel column using 15/85 methanol/DCM as eluent to get semisolid product. Yield = 5.4 g (67%). ^{1}H NMR (d_6-DMSO) δ: 7.17 ppm (m, 2H, Ar—H), 6.83 ppm (d, 2H, Ar—H), 3.89 ppm (t, 2H, Ar—O—CH_2), 2.49 ppm (t, 2H, HO_3S—CH_2), 1.72 ppm(b, 4H, CH2—CH_2—CH_2—CH_2—SO_3H), 1> (m, aliphatic side chain). ^{13}C NMR (d_6-DMSO) δ: 156.2, 156.1, 1.41.7, 139.3, 138.9, 127.4, 126.8, 126.7, 113.6, 113.5, 69.6, 67.1, 67.0, 51.2, 28.1, 22.0, 13.9, 11.1, and 8.6. FT-IR (KBr): 3417, 2958, 28721656, 1580, 1467, 1365, 1246, 1185, 1054, 957, 828, 731, 669, 613, and 530. MALDI-TOF-TOF (MW: 365.3): m/z = 395.0 (as MK^+ ion).

Synthesis of 3-(2-nonylphenoxy)propane-1-sulfonic acid (NON-C3)

1,3-propanesultone (5.5 g, 45.4 mmol) was ring opened by Nonyl phenol (5.0 g, 22.7 mmol) in presence of base potassium tertiarybuoxide (5.1 g, 45.4 mmol) in dry ethanol (50 mL) following the reaction procedure described for PDP-C4. The crude solid was purified by passing through a silica gel column using 15/85 methanol/DCM as eluent to get semisolid product. Yield = 7.5 g (97%) ^{1}H NMR (d_6-DMSO) δ: 7.17 ppm (m, 2H, Ar—H), 6.83 ppm (d, 2H, Ar—H), 3.90 ppm (t, 2H, Ar—O—CH_2), 2.49 ppm (t, 2H, HO_3S—CH_2), 1.91 ppm(b, 4H, CH2—CH_2—CH_2—SO_3H), 1> (m, aliphatic side chain). ^{13}C NMR (d_6-DMSO) δ: 156.2, 141.7, 140.9, 138.9, 127.4, 126.8, 126.7, 113.7, 69.0, 66.7, 66.4, 48.0, 39.0, 38.8, 25.3, 14.1, 11.3, and 8.5. FT-IR (KBr): 3544, 3479, 2916, 2853, 1618, 1579, 1471, 1471, 1445, 1298, 1246, 1183, 1061, 970, 869, 774, 749, 723, 690, 684, 621, 588, and 524. MALDI-TOF-TOF (MW: 342.5): m/z = 381.0 (as MK^+ ion).

Preparation of Polyaniline Nanomaterial via Emulsion Route

Typical procedure for the emulsion polymerization for polyaniline nanomaterial is explained in detail for PDP-C4 assisted process. Similar synthetic procedure is adopted for other dopants unless specified separately. PDP-C4 (97 mg, 0.22 mmol for 1 : 1/50 composition) was taken in distilled water (20 mL) and stirred under sonication for 15 min. Distilled aniline (1.0 mL, 11.0 mmol) was added to the surfactant solution and stirred under sonication for 1 h. At the end of sonication, the polymerization mixture turned into a pale yellow thick emulsion. APS (1.35 M aqueous solution, 5.0 mL) was added dropwise at 0°C to the above solution and continued the stirring under sonication for 1 h. The polymerization was continued without disturbance for 15 h at 5°C. The polymer was filtered, washed with water and methanol till the filtrate become colorless. The green polymer was dried under vacuum oven for 24 h at 60°C (0.01 mmHg). Yield = 240 mg (24%). ^{1}H-NMR (400 MHz, d_6-DMSO) δ: 7.40 ppm (m, 2H, Ar—H, Pani), 7.44 ppm (m, 2H, Ar—H, Pani), and 7.78 ppm (s, 4H, Ar—H Dopant). FT-IR (KBr, cm^{-1}): 1570, 1500, 1300, 1140, 1030, 818, and 694. UV-visible (in water, nm) λ max: 297, 427, and broad peak at 838 nm.

The same procedure was adopted for synthesis of polyaniline by using rest of the five dopants PDP-C3, CAR-C4, CAR-C3, NON-C4, and NON-C3 for 1 : 1/50 composition.

Applied Polymer SCIENCE

Dispersion Route for Polyaniline Nanomaterials

Typical procedure for the dispersion polymerization for polyaniline nanomaterial is explained in detail for PDP-C4 assisted process. Similar synthetic procedure is adopted for other dopants unless specified separately. PDP-C4 (97 mg, 0.22 mmol for 1 : 1/50 composition) was taken in distilled water (20 mL). In a separate glass vial, distilled aniline (1.0 mL, 1.02 g, 11.0 mmol) was dissolved in toluene (10 mL). To the dopant solution, aniline in toluene was added and the mixture was sonicated for 1 h to obtain a milky white dispersion. APS solution (1.35 M, 5.0 mL) was added to the dispersion and stirred under ultrasonic for 10 min at 30°C. The polymerization was allowed to continue at 5°C for 15 h without further disturbance. The dark green polyaniline solid mass was filtered, washed with distilled water and methanol several times until the filtrate become colorless. The solid product was dried in a vacuum oven at 60°C for 48 h (0.01 mmHg). Yield = 243 mg (25%). ^{1}H-NMR (400 MHz, d_6-DMSO) δ: 7.40 (m, 2H, PANI), 7.44 (m, 2H, PANI), and 7.78 (s, 4H, Ar—H Dopant). FT-IR (KBr, cm^{-1}): 1570, 1500, 1300, 1140, 1030, 818, and 694. UV-visible (in water, nm) λ max: 313, 417, and broad peak at 848 nm.

The same procedure was adopted for synthesis of polyaniline by using rest of the five dopants PDP-C3, CAR-C4, CAR-C3, NON-C4, and NON-C3 for 1 : 1/50 composition.

Interfacial Polymerization of Polyaniline Nanaomaterials

Typical procedure for the interfacial polymerization for polyaniline nanomaterial is explained in detail for PDP-C4 assisted process. Similar synthetic procedure is adopted for other dopants unless specified separately. PDP-C4 (97 mg, 0.22 mmol for 1 : 1/50 composition) was taken in distilled water (30 mL). In a separate glass vial distilled aniline (1.0 mL, 1.02 g, 11.0 mmol) was dissolved in dichloromethane. To the dichloromethane solution, dopant plus oxidant in water was carefully added without disturbing the interface. The interfacial polymerization was allowed to stand at 5°C for 15 h without disturbing. Then the polyaniline solid mass was formed in the aqueous phase which was centrifuged and washed with distilled water and methanol several times until the filtrate become colorless. The solid product was dried in a vacuum oven at 60°C for 24 h (0.01 mmHg). Yield = 72 mg (73%). FT-IR (in cm^{-1}): 1570, 1480, 1300, 1110, 802, 694, and 617. UV-visible (in water, nm) λ max: 328, 449 and free carrier tail >700.

The same procedure was adopted for synthesis of polyaniline by using rest of the five dopants PDP-C3, CAR-C4, CAR-C3, NON-C4, and NON-C3 for 1 : 1/50 composition.

RESULTS AND DISCUSSION

The synthesis of new amphiphilic dopants are described in Figure 1. Pentadecylphenol, cardanol, and nonyl phenol have unique in-built long hydrophobic alkyl tail attached in the aromatic ring. All there phenols are vary in the length (9 or 15 carbon atoms), nature (saturated or unsaturated), and position of the attachment at the aromatic ring of alkyl chain (ortho or meta). The phenols were reacted with 1,4-butanesultone and 1,3-propanesultone to make six structurally different dopants as shown in Figure 1. The dopant molecules behave as typical

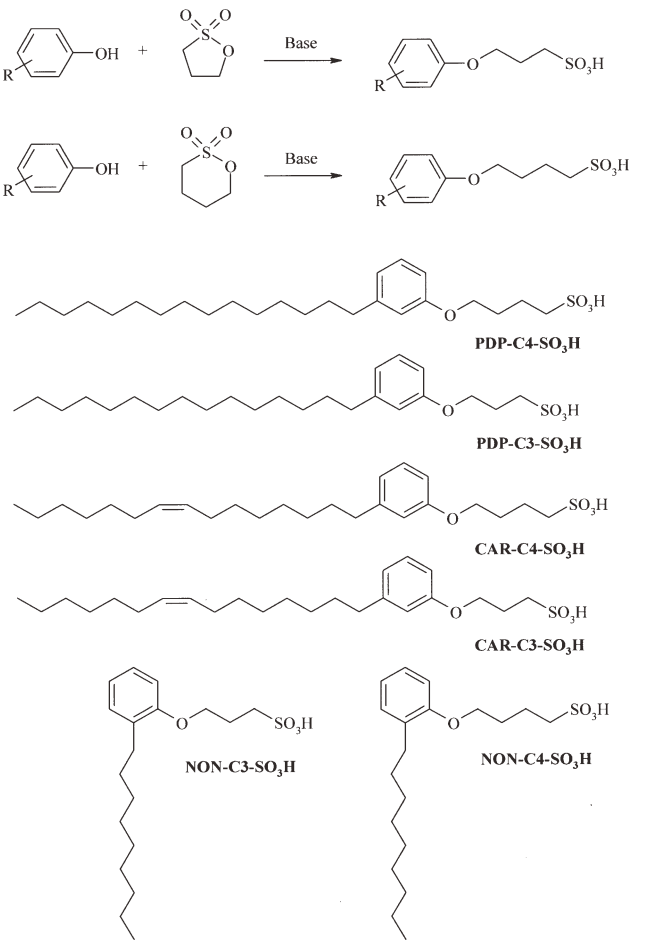

Figure 1. Synthesis of amphiphilic sulfonic acid dopants via ring opening of sultone.

amphilphiles through hydrophilic sulphonic acid as a polar head and the long alkyl chain as a hydrophobic tail. The dopants are named as AAA-Cn, where AAA = represents their phenol origin (PDP = pentadecyl, CAR = cardanol, NON = nonyl) and "*n*" represents the number carbon atoms (either 3 or 4) between the aryl to —SO_3H unit in the dopant structure. The purity and structure of the dopants were confirmed by NMR, FT-IR, and MALDI (see supporting information).

The dopants are highly soluble in water and forms foam at the water air interface indicating the typical surfactant like behaviors. To understand self-assembly of the dopant molecules; aqueous solution of dopants at various concentrations were subjected to three different independent techniques such as DLS, Zeta potential, and surface tension. DLS histograms of the all six amphiphilic dopants are provided in supporting information. DLS plots showed single distribution for all the dopants with the formation of uniform micelles in the range of 3–6 nm in size. The plots of concentrations versus the sizes of the nanoaggregates are shown in Figure 2a. The critical micelle concentrations (CMC) of the dopants were obtained from the break points in the plots and the values are summarized in Table I. For example, PDP-C4 showed sharp break point at 1×10^{-4} M concentration which is corresponding to its CMC in water. The

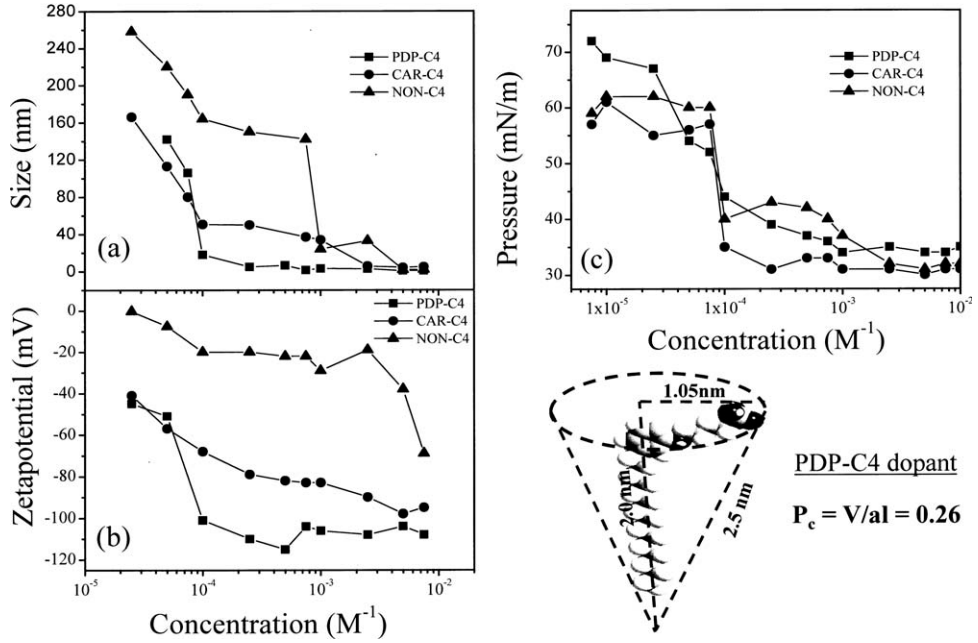

Figure 2. DLS size data (a), zeta potential (b), and surface tension (c) of dopants at various concentrations in water. The packing parameter (P_c) is determined for dopant PDP-C4.

plot corresponding to NON-C4 dopant showed two break points at 1×10^{-4} (weak aggregation) and 1×10^{-3} M^{-1} (strong aggregation). The CMC was determined from the second break point. Zeta potential measurement is very important tool for understanding the solution dynamic of charged particles or aggregates. Charged species tend to move under the influence of an electric field and the electrical potential at the surface of the sphere of radius "a" and carrying charge q is: $\zeta = q/4\pi\varepsilon a$, where ζ and ε are zeta potential and permittivity of the medium in which they are immersed.[35] The zeta potential for the various concentrations of the AAA-C4 series dopants are recorded and the results are plotted in Figure 2b. All the three plots in the zeta potential versus concentration showed a nonlinear trend with break points at closer to the CMC values determined by DLS techniques. As expected for sulfonic acids, the zeta potential of the dopant micelles possessed negative charges, however, their magnitude vary with the types of the structures. Based on the equation expressed above, the Zeta potential is typically inversely proportional to the size of the aggregates and therefore, a larger particle expected to show less zeta potential and vice versa. The comparison of the size distribution and zeta potential graphs revealed that NON-C4 dopant has larger size and as result showed lower zeta potential values. The stability of the charged colloids increases with increase in the Zeta potentials. Therefore, the stability of the smaller and tiny PDP-C4 and CAR-C4 micelles are much higher compared to that of the larger NON-C4 dopants in water (negative sign indicates only the charge of the species and stability should be correlated to the magnitude). The sharp break points are corresponding to the CMC of the dopants and the values are reported in Table I. Further to confirm the CMC values, we have carried out concentration dependent surface tension measurement by using Langmuir-Blodgett method in water. Surface tension values were plotted against concentration of dopant of AAA-C4 series as shown in Figure 2c. Below the CMC, surface tension decreases with increase in surfactant (or dopant) concentration. The CMC is obtained at concentration where the surface tension trend changes and become constant. The CMC obtained by surface tension for all the dopants are given in the Table I. Interestingly, the NON-C4 dopant showed two break points corresponding to weak and strong self-organization in both Zeta potential and surface tension methods as similar to the DLS data.

The critical packing parameter (P_c) directly correlates the expected geometry of amphiphilic molecule self assembly for spherical micelles ($P_c = <0.33$), cylindrical micelles ($P_c = 0.33$–0.50), bilayers ($P_c = 0.50$–1.0), and reverse or inverted micelles ($P_c > 1$).[36] The critical packing parameter (P_c) could be determined based on the equation, $P_c = V/al$ where V is volume occupied by hydrophobic part of molecule, "a" is the area of

Table I. Critical Micelle Concentration and Packing Parameter of Dopants

Sample	CMC by DLS[a]	CMC by ZP[b]	CMC by ST[c]	P_c[d]
PDP-C4	1.0×10^{-4}	1.0×10^{-4}	1.0×10^{-4}	0.266
CAR-C4	2.5×10^{-3}	1.0×10^{-3}	1.0×10^{-3}	0.288
NON-C4	7.5×10^{-4}	2.5×10^{-3}	2.5×10^{-3}	0.444
PDP-C3	-	5.0×10^{-4}	5.0×10^{-4}	0.359
CAR-C3	-	7.5×10^{-4}	2.5×10^{-4}	0.309
NON-C3	-	1.0×10^{-3}	7.5×10^{-4}	0.402

[a]Determined by dynamic light scattering in water at 30°C, [b]Determined by zeta potential in water at 30°C, [c]Determined by surface tension method in water at 30°C, [d]Calculated based on energy minimize structure.

Table II. Properties of Emulsion, Dispersion, and Interfacial Polymers

Sample	Dopant in feed (in M)	σ^a (S/cm)	$\eta_{inh}{}^b$ (dL/g)	WXRD^c (2θ)	$T_D{}^d$ (°C)
PDPC4E	1.1×10^{-2}	8.34×10^{-5}	0.10	6.5, 19.2, 25.9	262
PDPC3E	1.1×10^{-2}	6.30×10^{-5}	0.17	6.5, 19.2, 25.9	261
CARC4E	1.0×10^{-2}	1.95×10^{-5}	0.17	6.5, 19.2, 25.9	263
CARC3E	1.0×10^{-2}	6.08×10^{-5}	0.27	6.5, 19.2, 25.9	252
NONC4E	1.0×10^{-2}	5.82×10^{-5}	0.22	6.5, 19.2, 25.9	253
NONC3E	1.0×10^{-2}	4.91×10^{-5}	0.10	6.5, 19.2, 25.9	245
PDPC4D	1.1×10^{-2}	2.13×10^{-4}	0.09	6.2, 22.8, 29.3, 20.5	218
PDPC3D	1.1×10^{-2}	2.84×10^{-3}	0.06	6.2, 22.8, 29.3, 20.5	222
CARC4D	1.0×10^{-2}	6.04×10^{-4}	0.04	6.2, 22.8, 29.3, 20.5	226
CARC3D	1.0×10^{-2}	1.27×10^{-3}	0.09	6.2, 22.8, 29.3, 20.5	223
NONC4D	1.0×10^{-2}	9.39×10^{-4}	0.05	6.2, 22.8, 29.3, 20.5	234
NONC3D	1.0×10^{-2}	5.13×10^{-3}	0.05	6.2, 22.8, 29.3, 20.5	213
PDPC4I	1.1×10^{-2}	1.30×10^{-2}	0.13	6.0, 18.3, 20.0, 25.5	191
PDPC3I	1.1×10^{-2}	8.15×10^{-3}	0.22	6.0, 18.3, 20.1,	192
CARC4I	1.0×10^{-2}	1.19×10^{-2}	0.15	6.0, 18.3, 24.0,	256
CARC3I	1.0×10^{-2}	1.07×10^{-2}	0.17	6.5, 19.3, 25.5	261
NONC4I	1.0×10^{-2}	1.49×10^{-2}	0.16	6.1, 20.1, 25.5	262
NONC3I	1.0×10^{-2}	1.52×10^{-2}	0.15	6.4, 20.4, 25.5	190

[a]Four probe conductivity at 30°C, [b]Solution viscosity of polymer for concentration 0.5 g/dL in N-methylpyrrolidone at 30°C, [c]Powder X-ray data at 30°C, [d]Thermal decomposition at 10% weight loss.

head group, and l is the length of molecule.[37] To calculate P_c, we have utilized energy minimized MM2 structure of all six dopants by using "Gaussian" software. We have measured critical packing parameter for all six dopants and values are provided in Table I. Critical packing parameter for PDP-C4 (P_c = 0.266) and CAR-C4 (P_c = 0.288) are below 0.33 which indicates the formation of spherical micelles. Critical packing factor obtained for NON-C4 (0.444) is much higher than other two dopants in the C-4 series and the P_c value is found corresponding to cylindrical micelles rather than spherical micelles. It suggested that the two break points in the CMC plots for NON-C-4 could arise due to this abnormal self-organization of the sulfonic acid dopant. The reason for the difference in the self-organization of NON-C4 is attributed to the variation in its chemical structure compared to PDP-C4 (also CAR-C4). The CMC of AAA-C3 series were also determined by methods described above (see supporting information) and their values are summarized in Table I. AAA-C3 series produced tiny micelles; however, DLS and zeta potential techniques are not adequate enough to get good CMC values. Surface tension method produced very good nonlinear trend and the CMCs for AAA-C3 series were determined. The CMC (one order of magnitude) and P_c values of the AAA-C3 dopant series were found much higher compared to that of AAA-C4 series suggesting that the alkyl unit between the aryl and sulfonic acid units are very crucial factor in the self-organization of dopants. The C-4 units produced better self-organized and stable structures compared to that of the C-3 units. The position of the attachment of the alkyl chain at the aromatic units is also important factor. For example, metasubstitution produced better packing than the orthosubstitution and the difference is attributed to the steric hindrance. The above detail analysis revealed that structural design of the dopant is very important to get appropriate molecular self-organization in water.

All six anionic dopants were employed as dopant-cum-surfactants for making polyaniline nanomaterials in three different polymerization routes such as emulsion, interfacial, and dispersion. Based on our previous experience in the polyaniline nanomaterial synthesis,[23] the composition of monomer to dopant [aniline]/[surfactant] was fixed as 1 : 1/50 i.e., 50 times lower amount of dopant compared to the concentration of aniline employed for the polymerization. In the emulsion polymerization, dopant+aniline was taken in 20 mL of water and subjected to sonication for 15 min to form thick emulsion. These emulsion mixtures were polymerized by adding aqueous solution of ammonium persulphate in ice cold condition and keeping the reaction mixture without any disturbance for overnight at 5°C. The resultant dark green material was filtered, washed with water and methanol until the filtrate became colorless. The polymers are denoted as AAA-Cx-E. In case of dispersion polymerization, the dopant was taken in 20 mL distilled water and subjected to sonication for 15 min. In a separate glass vial, distilled aniline was dissolved in 10 mL toluene. To the dopant solution, aniline in toluene was added and the mixture was subjected to sonication for 1 h to obtain a milky white dispersion. The white thick dispersion was polymerized by adding APS solution in cold condition. The polymerization was allowed to continue at 5°C for 15 h without further disturbance. The dark green polyaniline solid mass was filtered, washed with distilled water and methanol several times until the filtrate become colorless. Polymers obtained by dispersion route are denoted by

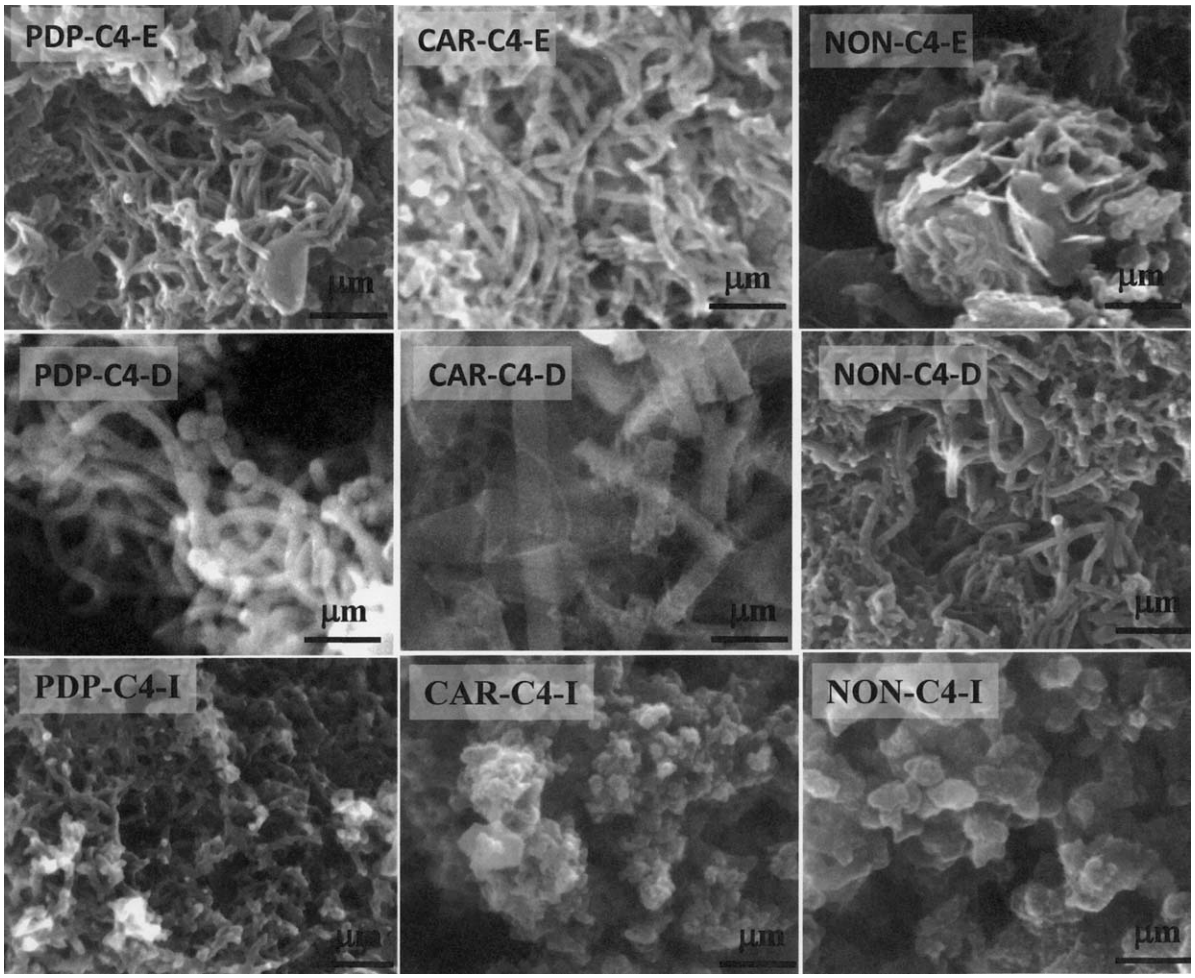

Figure 3. SEM images of PANI nanomaterials.

AAA-Cx-D. Interfacial polymerization was the third method used for polyaniline nanomaterial synthesis in which dopant was taken in 30 mL distilled water. In a separate glass vial, distilled aniline was dissolved in dichloromethane. To the dichloromethane solution, dopant plus oxidant in water was carefully added without disturbing the interface. The interfacial polymerization was allowed to stand at 5°C for 15 h without disturbing. Then green colored polyaniline solid mass in the aqueous phase which was centrifuged. It was filtered and washed with distilled water and methanol several times until the filtrate become colorless. Polyaniline samples obtained by interfacial route are denoted by AAA-Cx-I. All the polymer samples were dried in a vacuum oven at 60°C for 48 h (0.01 mm of Hg). All polyaniline samples were subjected for FT-IR analysis for structural characterization and their spectra were matched with earlier reports[38] (see supporting information). Thermal stability of the nanomaterials was determined by TGA and thermograms are provided as supporting information. All polymer nanomaterials synthesized via three different synthetic route shows two steps thermal decomposition. First 10% weight loss was observed at temperature lower than 280°C followed by second decomposition at 460°C (see Table II). Inherent viscosity was recorded for all polymeric samples in N-methylpyrrolidone solvent at 30°C. Both interfacial and emulsion route synthesized nanomaterials showed inherent viscosities η_{inh} = 0.1–0.22 dL/g in NMP for 0.5 wt % polymer solutions which are in accordance with the reported values.[39,23] Dispersion route synthesized samples showed less viscosity η_{inh} = 0.05–0.09 dL/g compared to the other two polymerization routes.

The morphology of the nanomaterials was recorded using SEM and images for AAA-C4 series are shown in Figure 3. The morphology of nanomaterials synthesized by PDP-C4 dopant produced thick and long nanofibers irrespective of the polymerization routes. The fibers were obtained with length up to 3–4 μm and width of about 150 ± 10 nm. The nanofibers produced by the interfacial route found shorter and thinner (70 nm thick and 0.5 μm length). The nanomaterials morphology of the samples produced by the unsaturated tail surfactant (CAR-C-4) was found highly sensitive to the types of the polymerization route. The morphologies were obtained as nanofibers, nanotapes, and nanosphers for emulsion, dispersion, and interfacial routes, respectively. The nonyl chain surfactant NON-C-4 produced flake-like morphology in the emulsion route. The dispersion and the interfacial routes produced fibers and spheres, respectively. The SEM images of the samples revealed that the

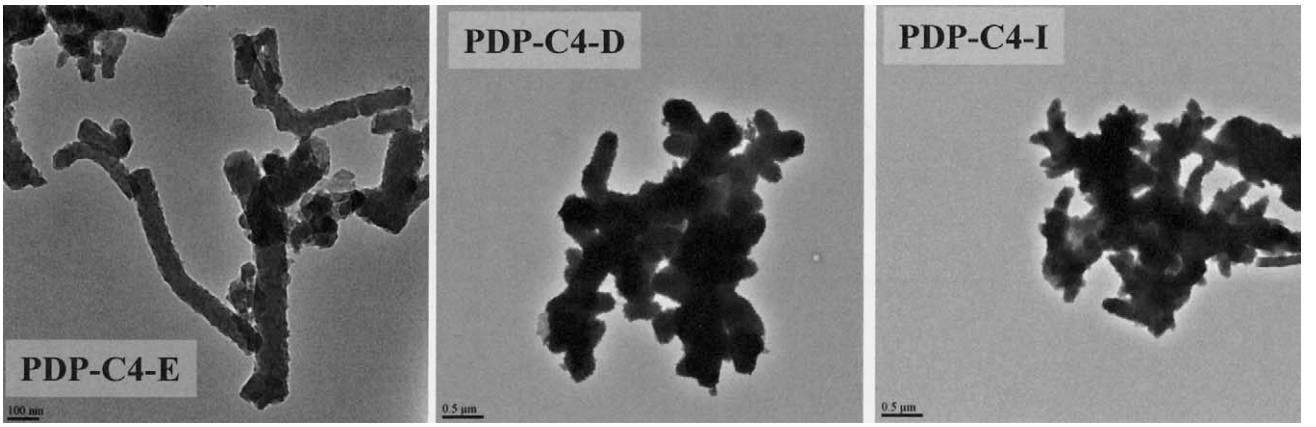

Figure 4. TEM images of PANI nanomaterials.

nanostructure morphology of the polyanilines based on CAR-C4 and NON-C4 are highly dependent on the polymerization routes. On the other hand, the PDP-C4 dopant produced same nanofibers in all three polymerization routes. TEM images of PDP-C-4 nanomaterials are shown in Figure 4. Emulsion, dispersion, and interfacial route clearly confirm the formation of solid nanomaterials and their images are in accordance with their SEM analysis. Hence, both the structure of the surfactant and polymerization route are determined the morphology of the polyaniline nanostructures.

Absorbance spectra of polyaniline nanomaterials were recorded by dispersing the nanomaterials in water which are shown in Figure 5. Amphiphilic nature of the surfactants enhances the dispersion stability of the nanomaterials in water. Emulsion and dispersion route synthesized polyaniline nanomaterials showed three transitions at 300 nm, 420 nm, and a broad peak at 850

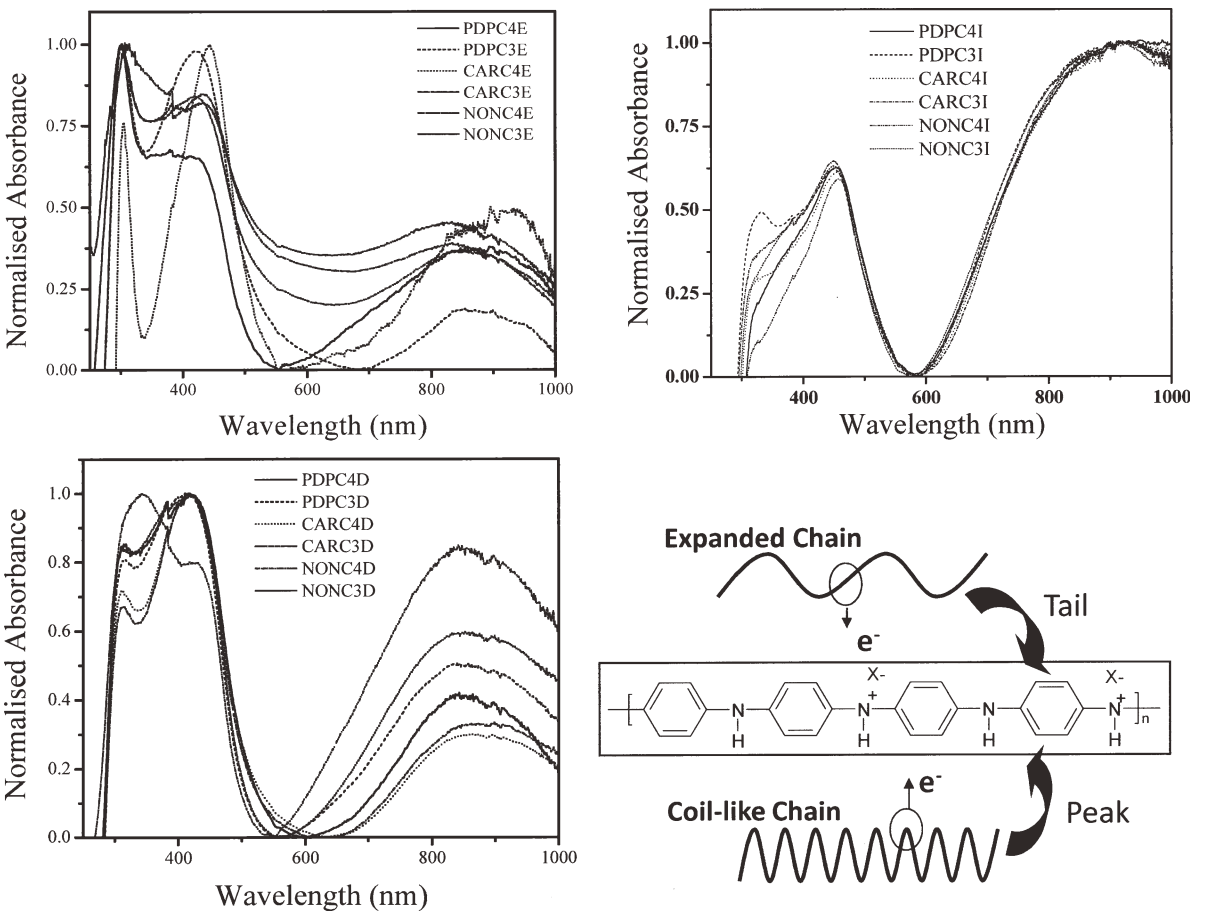

Figure 5. Absorption spectra of polyaniline nanomaterials in water at 30°C.

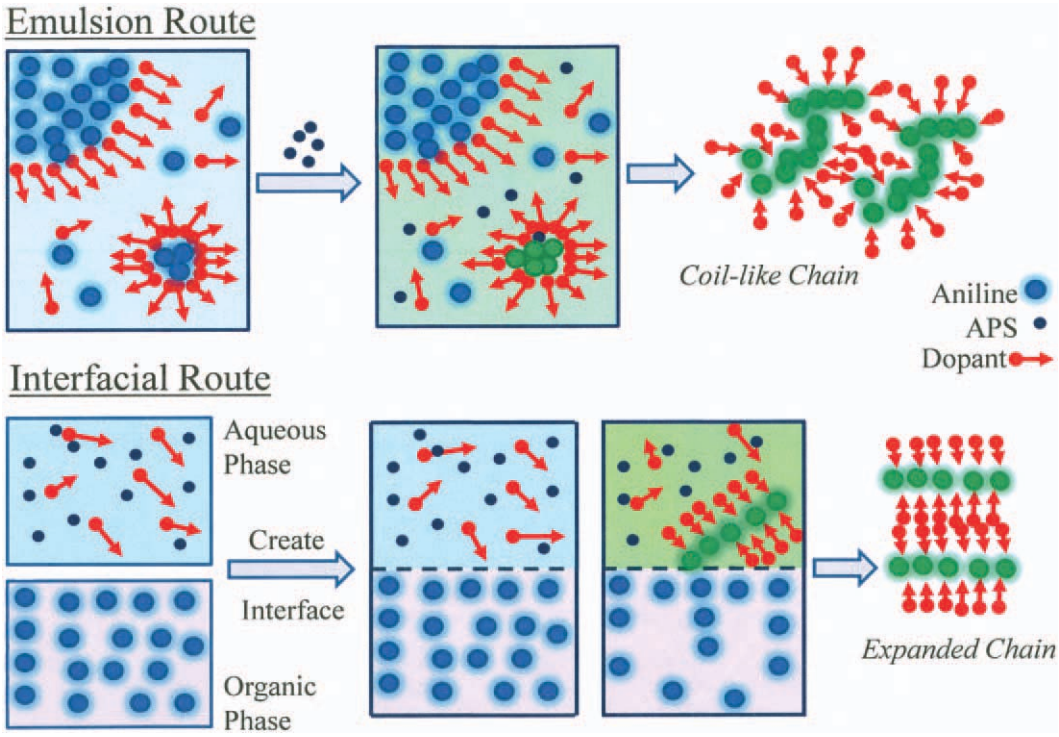

Figure 6. Mechanism of nanofiber formation and their respective chain conformation. [Color figure can be viewed in the online issue, which is available at wileyonlinelibrary.com.].

nm with respect to π–π^* transition, polaron to conducting band, valence band to polaron band, respectively.[40] Polyaniline nanomaterials synthesized via interfacial route showed same absorption spectra except free carrier tailing above 800 nm with high optical density than emulsion and dispersion route synthesized nanomaterials. The emulsion and dispersion route synthesized polyanilines possessed broad peak maxima at 800 nm whereas tail-like features are observed in the case of interfacial samples. The appearance of peak and tail-characteristics in the near-IR region above 850 nm are assigned to the delocalization of polaron band with respect to coil-like or expanded conformation in the polyaniline chains, respectively.[28–30,23c,d] Therefore, the polymer nanomaterials produced by the emulsion and dispersion routes possessed coil-like conformation whereas expanded chains are obtained in the interfacial route. The conformational changes in polyaniline nanomaterials actually arise from their difference in mode of chemical reactions in polymerization process. Schematic representation of the polymerization of aniline in the presence of the sulfonic acid dopants are shown in Figure 6. In the emulsion polymerization, there are two types of aggregates are possible: (i) larger micrometer size oil drops stabilized by the dopants and (ii) small nanoreactors constituted by the tiny micelles of the dopants. The larger surface area to volume ratio in the tiny micelles attract the sulfonate radical anion initiator [$SO_4^-\cdot$, produced by the disassociation of $(NH_4)_2S_2O_8$ in water].[41] Subsequently, the polymerization proceeds in the aniline molecules present in the hydrophobic middle core. The charged polyaniline chains possessed higher affinity towards water; as the consequence, the micelles dissociate and the polymers get absorbed in water. The dopant molecules again associate to form new micelles with aniline supplied form the big oil droplets encapsulated in the hydrophobic core and new reaction starts and so on. In the interfacial synthesis, the aniline monomers get absorbed at the aqueous-organic interface and get oxidized by the APS present in the aqueous medium. The high water affinity of the polymer chains enhances their presence in water rather than in organic phase. At the interface, new reaction cites are created for growing new polymer chains and the process continuous till the end of the polymerization. As a net effect, the interfacial route provides aniline monomers unidirectional chain growth at the interface. Dispersion route is almost similar to emulsion polymerization; however, the reaction sites are not tiny micelles rather than big oil drops.[41] Hence, both emulsion and dispersion routes do not provide unidirectional growth pathways for the polymer chains unlike in the case of interfacial route. The polymer chains grow with directionality arranged in the expanded conformation (interfacial route) whereas the coil-like conformations are obtained in emulsion and dispersion routes. The expanded conformation showed tail-like features in the near IR region whereas peaks are observed for coil-like conformation (see Figure 5).

To study the influence of the expanded and coil-like conformation on the packing of the polyanilines nanomaterials in the solid-state, the samples were subjected to WXRD. WXRD patterns of the samples synthesized all three routes for C-4 series are given in Figure 7 (see Table 2). Anionic amphiphilic dopant can induce electrostatic interaction with polymer chain which organizes the polymer chains in three-dimensional and highly

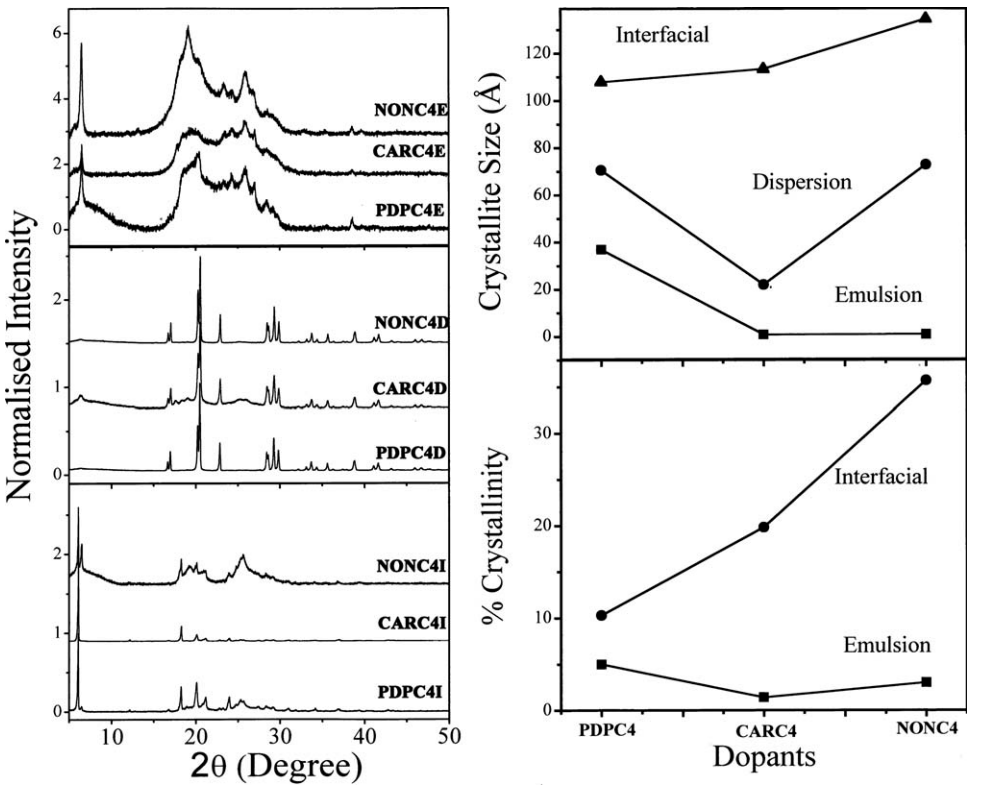

Figure 7. Wide angle X-ray diffraction pattern of polyaniline nanomaterials and plots of percent crystallinity and crystallite size versus amphiphilic dopants in emulsion and interfacial routes.

ordered states. Emulsion route synthesized polymers showed broad peaks at $2\theta = 19.2$ (d-spacing = 4.6 Å) and $2\theta = 25.9$ (d-spacing = 3.4 Å) corresponding to aromatic chain interaction.[42,23b,d] These nanomaterials also showed lower angle peak at $2\theta = 6.5$ (d-spacing = 13.5 Å) attributed to interdigitation of long tail substituted dopants into the polyaniline matrix. Dispersion route synthesized nanomaterials showed at higher angle peak at $2\theta = 22.8$ and 29.3 corresponding to aromatic interactions as similar to that of emulsion route samples.[23] However, the dispersion route samples did not show any peak at low angle at $2\theta = 6.2$ (unlike in the emulsion route) which suggested that the dispersion route synthesized polyaniline nanomaterials have weak short range ordering in the nanomaterials. In case of interfacial route, the polyaniline nanomaterials showed difference in their WXRD patterns depending upon their type of the amphiphilic dopants used for the synthesis. The samples synthesized by the PDP and CAR-based dopants showed highly ordered sharp lower angle peak at $2\theta = 6.5$ (d-spacing = 13.5 Å). Presence of intense lower angle peak indicates high solid state ordering in the polyaniline nanomaterials. In the case of the NON-dopant, broad peaks are obtained with respect to less crystalline character compared to other two dopants. WXRD studies provide direct evidence that the samples produced by the interfacial route samples possessed superior solid state ordering compared to that of the emulsion and dispersion routes. The percent crystallinities and crystallite size (L) were determined by the TOPAZ programme based on the WXRD data. The crystallite size (L) was determined using the formula: $L = 0.9\ \lambda/\beta\ \cos\theta$, where λ is the source wavelength, β is full width at half maximum, and θ angle of the measurement.[43,44] The percent crystallinity was determined by taking the ratio of sharp peaks in the crystalline domain to the crystalline + amorphous domains.[44] The absences of the low angle sharp peak in the dispersion route samples limit their percent crystallinity determination under identical conditions. The percent crystallinity and L values are plotted and shown in Figure 7. The samples synthesized via interfacial route showed high percent crystallinity compared to those obtained via emulsion route. The L-values follow the order: emulsion < dispersion < interfacial indicating that the interfacial route samples are highly ordered in the solid state compared to other routes. Hence, it is very clearly evident that the expanded conformation (based on absorbance spectra, see Figure 5) in the interfacial samples produced highly ordered polymer chains.

To study the role of the conformation and the solid state ordering of the polyaniline nanomaterials on the conductivity behaviors, the samples were subjected to four probe method using kethley's current and nanovoltmeter source. The I-V measurements of the samples are carried out for 10 mm diameter and 1 mm thickness pellets and their plots are given in Figure 8. The slope of the I-V plot gives the resistivity of the sample and the inverse of the resistivity is corresponding to the conductivity. The conductivities of the samples are plotted and shown in Figure 8. Emulsion route synthesized nanofibers showed conductivity in the range of 10^{-5} S/cm for all the samples irrespective of

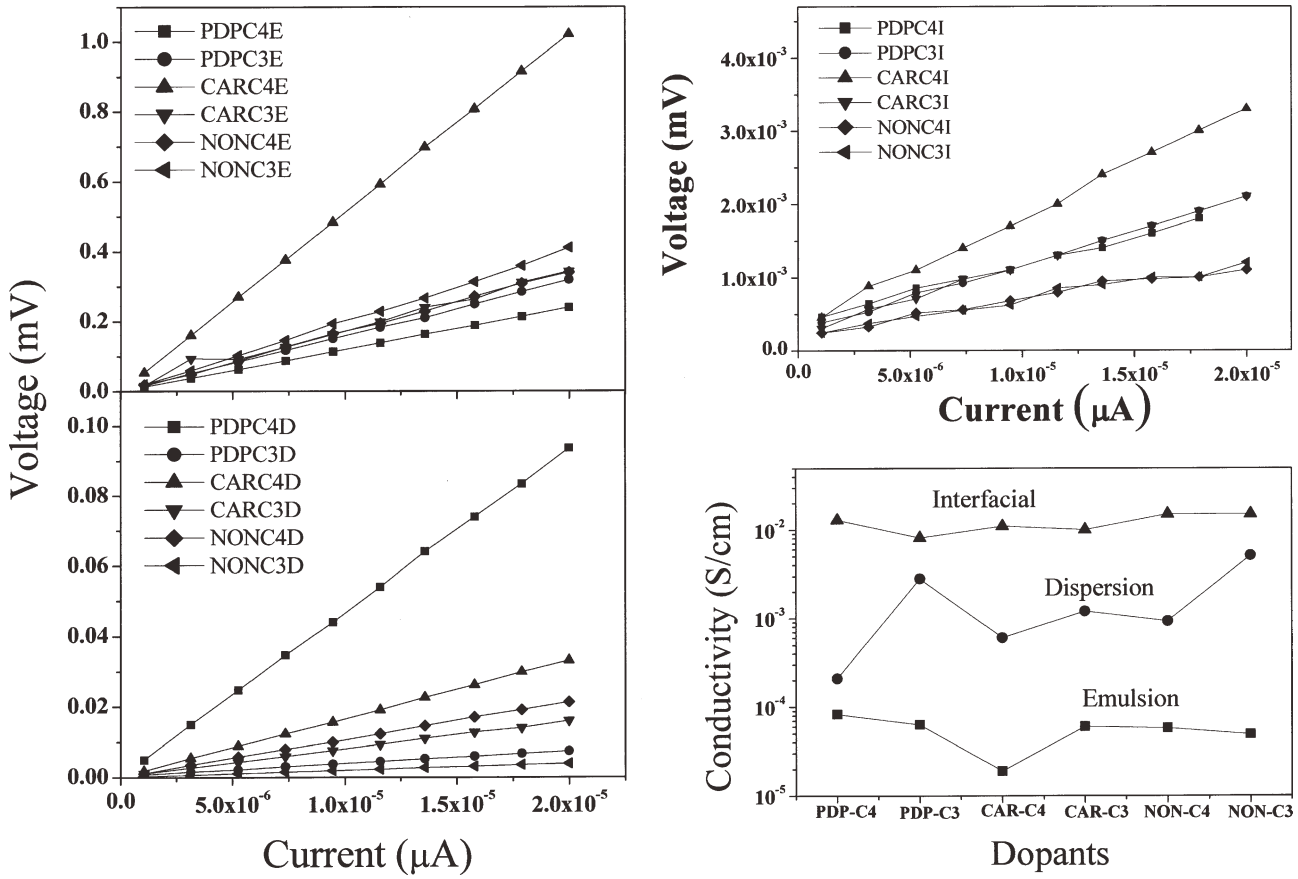

Figure 8. I-V plots of polyaniline nanomaterials and plots of conductivity versus types of amphiphilic dopants in various polymerization routes.

the dopant employed for the synthesis (see also Table 2). The conductivity of the dispersion route samples were obtained in the average of 6×10^{-4} S/cm. Interestingly, the interfacial route samples produce very high conductivity in the range of 1×10^{-2} S/cm. The reason for the low conductivity in the emulsion route synthesized samples (10^{-3} S/cm) are attributed to the usage of less amount of dopant (50 times lower amount of dopant compared to aniline) in the nanofiber synthesis.[23b,d] Nevertheless, the conductivities of the polymer samples were matched with the reported values for sulfonic acid-based nanomaterials.[34c,45,46] The conductivities of the interfacial route samples are obtained very high irrespective of the dopant employed or difference in the morphologies among of the samples (see SEM image in Figure 3). Further, the emulsion route samples produced similar fibrous morphology; however, their conductivities vary largely dependent on the polymerization route. Therefore, the conductivities of the polyaniline samples are mainly controlled by the factors other than the morphologies. In the present case, the conformation of the polymer chains and the crytallinity associated with the samples primarily determine the properties such as solid state ordering and conductivity. Though, the dispersion and emulsion route methodologies are very good for large scale production, further studies are required to optimize the synthetic pathways or structure of the dopant molecules to make highly ordered and conducting samples. The newly designed amphiphilic dopant molecules are very efficient structure directing units for polyaniline nanomaterials and very useful for various polymerization routes like emulsion, dispersion, and interfacial. The unidirectional growth of the polymer chains in the interfacial route resulted in the formation of expanded conformation, highly ordered, and high conductivity of the samples. Hence, the conformation driven packing of the chains in the solid state is very crucial factor for the conductivity of the polymer chains, more exclusively polyaniline nanomaterials.

CONCLUSION

In conclusion, we have designed and developed six new structurally different amphiphilic sulfonic acid surfactant-cum-dopants for polyaniline nanomaterials. The structure of the dopants are robust in the sense that these molecules could be employed as dopants for more than one polymerization routes in water for tuning the shape, size and other characteristics of conducting polymers. The important novelties of the present approach may be summarized as follows: (i) three long chain substituted phenols such as 3-pentadecylphenol, unsaturated C_{15}-chain phenol (cardanol), and nonyl phenol were subjected to ring opening reaction with butyl and propyl sultone to make six structurally different amphiphilic dopants, (ii) the current molecular design provide structural variation on both the hydrophilic and hydrophilic part of the molecules which are exploited

templating polyaniline synthesis, (iii) the dopant molecules self-organized in water as tiny micelles and their CMC were determined by DLS, Zeta potential, and surface tension techniques, (iv) critical packing parameter (P_c) of the dopants were determined and correlated to molecular self-organization in water, (v) all the six dopants produced thick white emulsion and dispersion with aniline in water or water + toluene mixture, respectively, which were used as templates for polymerization, (vi) the interfacial polymerization was carried out using the new dopants in water/dichloromethane interface, (vii) SEM and TEM analysis revealed that the morphology of the polymer samples such are found highly sensitive to the dopant structure and polymerization routes, (viii) absorbance spectra of the emulsion and dispersion samples were found to show peak like characteristics in the near IR-region with respect to coil-like conformation, (ix) interfacial samples produced expanded polymer chains conformation as a result the absorbance spectra showed tail-like features in the IR region, (x) the expanded conformation produced high order and crystalline state in the interfacial route samples, (xi) the four probe conductivity results indicate very high conductivity in the interfacial samples (10^{-2} S/cm) compared to that of the dispersion (10^{-4} S/cm) and emulsion (10^{-5} S/cm) route samples, and (xii) the higher conductivity of the samples are correlated to the high solid state ordered chains produced via expanded chain conformations. In the present investigation, by careful choosing of the polymerization routes and rational design of the dopant structures, we demonstrate that chain conformation and solid state ordering are two important factors which control the conductivity characteristics of the conducting polymers, more specifically polyaniline nanomaterials.

ACKNOWLEDGMENTS

We thank Department of Science of Technology, New Delhi, India under Scheme: NSTI Programme-SR/NM/NM-42/2009 for financial support. The authors thank NCL for SEM and TEM analysis.

REFERENCES

1. (a) Huang, J.; Virji, S.; Weiller, B. H.; Kaner, R. B. *J. Am. Chem. Soc.* **2003,** *125*, 314. (b) Huang, J.; Virji, S.; Weiller, B. H.; Kaner, R. B. *Chem. Eur. J.* **2004,** *10*, 1314. (c) Jeon, I.-Y.; Kang, S.-W.; Tan, L.-S.; Beak, J. B. *J. Polym. Sci. Polym. Chem.* **2010,** *48*, 3103. (d) Mahanta, D.; Madras, G.; Radhakrishnan, S.; Patil, S. *J. Phys. Chem. B.* **2009,** *113*, 2293.
2. (a) Cosnier, S. *Electroanalysis* **2005,** *17*, 1701. (b) Leclerc, M. *Adv. Mater.* **1999,** *11*, 1491.
3. Ko, S.; Jang, J. *Biomacromolecules* **2007,** *8*, 182.
4. (a) Anilkumar, P.; Jayakannan, M. *Langmuir* **2008,** *24*, 9754. (b) Antony, M. J.; Jayakannan, M. *Langmuir* **2011,** *27*, 6268.
5. (a) Manian, M. K.; Iyenagr, G. A.; Lee, K.-P.; Kim, N. H.; Shanmugasundaram, K.; Kang, S. H. *J. Polym. Sci. Polym. Chem.* **2010,** *48*, 4537. (b) Zhang, Y.-S.; Xu, W.-H.; yao, W.-T.; Yu, S.-H. *J. Phys. Chem. C.* **2009,** *113*, 8588. (c) Gao, C.; Ai, M.; Li, X.; Xu, Z. *J Polym. Sci. Polym. Chem.* **2011,** *49*, 2173. (d) Gizdavic-Nicolaidis, M. R.; Zujovic, Z. D.; Easteal, A. J.; Bowmaker, G. A. *J. Polym. Sci. Polym. Chem.* **2010,** *48*, 1339. (e) Deore, B. A.; Freund, M. S. *Macromolecules* **2009,** *42*, 164.
6. Skotheim, T. A.; Elsenbaumer, R. L.; Reynolds, J. R. Hand Book of conducting Polymers, 2nd ed.; Marcel Dekker: New York, **1997.**
7. Wu, A.; Kolla, H.; Manohar, S. K. *Macromolecules* **2005,** *38*, 7873.
8. Jang, J.; Oh, J. H.; Stucky, G. D. *Angew. Chem. Int. Ed.* **2002,** *41*, 4016.
9. Zhong, W.; Liu, S.; Chen, X.; Wang, Y.; Yang, W. *Macromolecules* **2006,** *39*, 3224.
10. Zhang, X.; Manohar, S. K. *Chem. Commun.* **2004,** 2360.
11. DeArmitt, C.; Armes, S. P. *Langmuir* **1993,** *9*, 652.
12. Omastova, M.: Trchova, M.; Kovarova, J.; Stejskal, J. *Synth. Met.* **2003,** *138*, 447.
13. Haung, K.; Wan, M.; Long, Y.; Chen, Z.; Wei, Y.; *Synth. Met.* **2005,** *155*, 495.
14. Bay, L.; Mogensen, N.; Skaarup, S.; Sommer-larsen, P.; jorgenson, M.; West, K. *Macromolecules* **2002,** *35*, 9345.
15. Liu, L.; Zhao, C.; Zhao, Y.; Jia, N.; Zhuo, Q.; Yan, M.; Jiang, Z. *Eur. Polym. J.* **2005,** *41*, 2117.
16. Menon, V. P.; Lei, J.; Martin, C. R. *Chem. Mater.* **1996,** *8*, 2382.
17. Ikegame, M.; Tajima, K.; Aida, T.; *Angew. Chem. Int. Ed.* **2003,** *42*, 2154.
18. Zhang, X.; Zhang, J.; Song, W.; Liu, Z. *J. Phys. Chem. B.* **2006,** *110*, 1158.
19. Shen, Y.; Wan, M. *Synth. Met.* **1998,** *96*, 127.
20. Wei, Z.; Zhang, L.; Yu, M.; Yang, Y.; Wan, M. *AdV. Mater.* **2003,** *15*, 1382.
21. Jayakannan, M.; Anilkumar, P.; Sanju, A. *Eur. Polym. J.* **2006,** *42*, 2623.
22. Jayakannan, M.; Annu, S.; Ramalekshmi, S. *J. Polym. Sci., Part B: Polym. Phys.* **2005,** *43*, 1321.
23. (a) Anilkumar, P.; Jayakannan, M. *Langmuir* **2006,** *22*, 5952, (b) Anilkumar, P.; Jayakannan, M. *J. Phys. Chem. C.* **2007,** *111*, 3591, (c) Anillkumar, P.; Jayakannan, M. *Macromolecules* **2007,** *40*, 7311. (d) Anillkumar, P.; Jayakannan, M. *Macromolecules* **2008,** *41*, 7706. (e) Anilkumar, P.; Jayakannan, M. *J. Phys. Chem. B.* **2009,** *113*, 11614. (f) Anilkumar, P.; Jayakannan, M. *J. Phys. Chem. B.* **2010,** *114*, 728. (g) Anilkumar, P.; Jayakannan, M. *J. Appl. Polym. Sci.* **2009,** *114*, 3531.
24. (a) Antony, M. J.; Jayakannan, M. *J. Phys. Chem. B.* **2007,** *111*, 12772. (b) Antony, M. J.; Jayakannan, M. *J. Polym. Sci. Part B Polym. Phys.* **2009,** *47*, 830.
25. (a) Antony, M. J.; Jayakannan, M. *J. Phys. Chem. B.* **2010,** *114*, 1314. (b) Antony, M. J.; Jayakannan, M. *J. Phys. Chem. B.* **2011,** *115*, 6427.
26. Zhang, Z.; Wei, Z.; Wan, M. X. *Macromolecules* **2002,** *35*, 5937.
27. Haung, J.; Kaner, R. B. *J. Am. Chem. Soc.* **2004,** *126*, 851.
28. MacDiarmid, A. G.; Epstein, A, J.; *Synth. Met.* **1995,** *69*, 85.
29. Min, Y.; Xia, Y.; MacDiarmid, A. G.; Epstein, A. *J. Synth. Met.* **1995,** *69*, 159.
30. Li, W.; Zhu, M.; Zhang, Q.; Chen, D. *Appl. Phys. Lett.* **2006,** *89*, 1031101.

31. Ma, H.-Y.; Luo, Y.-Q.; Yang, S.-X.; Li, Y.-W.; Cao, F.; Gong, J. *J. Phys. Chem. C.* **2011,** *115*, 12048.
32. Chattopadhyay, D.; Mandal, B. M. *Langmuir,* **1996,** *12*, 1585.
33. Armes, S. P.; Aldissi, M. Hawley, M.; Berry, J. G.; Gottesfeld, S.; *Langmuir* **1991,** *7*, 1447.
34. (a) Haung, K.; Wan, M. X. *Chem. Mater.* **2002,** *14*, 3486. (b) Zhang, X.; Goux, W. J.; Manohar, S. K. *J. Am. Chem. Soc.* **2004,** *126*, 4502. (c) Wei, Y.; Wan, M. X. *Adv. Mater.* **2002,** *14*, 1314.
35. Shaw, D. J. Introduction to Colloid and Surface chemistry; Butterworth Heinemann: Oxford, UK, **1992.**
36. Hamley, I. W. Introduction to Soft Matter, 2nd ed.; Wiley: New York, **2007; p 200.**
37. Shimizu, T.; Masuda, M.; Minamikawa, H. *Chem. Rev.,* **2005,** *105*, 1401.
38. Kang, E. T.; Neoh, K. G.; Tan, K. L. *Prog. Polym. Sci.* **1998,** *23*, 277.
39. Kim, B. J.; Oh, S. G.; Han, M. G.; Im, S. S. *Synth. Met.* **2001,** *122*, 297.
40. Xis, Y.; Wiesinger, J. M.; MacDiarmid, A. G. *Chem. Mater.* **1995,** *7*, 443.
41. Cowie, J. M. G. Polymers: Chemistry and Physics of Modern Materials, 3rd edn.; CRC press: UK, **2007; p 77.**
42. Lunzy, W.; Banka, E. *Macromolecule* **2000,** *33*, 425.
43. Pouget, J. P.; Jozefowicz, M. E.; Epstein, A. J.; Tang, X.; MacDiarmid, A. G. *Macromolecules* **1991,** *24*, 779.
44. Bhadra, S.; Khastgir, D. *Polym. Degrad. Stab.* **2007,** *92*, 1824.
45. Zhang, L.; Wan, M.; Wei, Y. *Macromol. Rapid Commun.* **2006,** *27*, 888.
46. Yang, C.-H.; Chih, Y.-K.; Cheng, H.-E.; Chen, C.-H. *Polymer* **2005,** *46*, 10688.